

# Low-temperature and hydrogen-free silicon dioxide cladding for next-generation integrated photonics

Zihan Li<sup>1,2,†</sup>, Zheru Qiu<sup>1,2,†</sup>, Rui Ning Wang<sup>3</sup>, Xinru Ji<sup>1,2</sup>, Marta Divall<sup>1,2</sup>, Anat Siddharth<sup>1,2</sup>, Tobias J. Kippenberg<sup>1,2,\*</sup>

<sup>1</sup>Swiss Federal Institute of Technology Lausanne (EPFL), CH-1015 Lausanne, Switzerland

<sup>2</sup>Center for Quantum Science and Engineering, EPFL, CH-1015 Lausanne, Switzerland

<sup>3</sup>Luxtelligence SA, CH-1015, Lausanne, Switzerland

\* E-mail: tobias.kippenberg@epfl.ch

**Abstract:** We demonstrate a process for hydrogen-free low-loss silicon oxide (SiO<sub>2</sub>) films deposited using SiCl<sub>4</sub> and O<sub>2</sub> as precursors. A wide low-loss window from 1260 nm to 1625 nm is achieved at a deposition temperature of 300 °C, essential for next generation photonic integrated circuits. © 2023 The Author(s)

## 1. Introduction

With the maturing of emerging low-loss integrated photonics platforms such as thin film lithium niobate (LiNbO<sub>3</sub>) on insulator [1], GaP on insulator and AlGaAs on insulator [2] and tantalum pentoxide (Ta<sub>2</sub>O<sub>5</sub>) [3], a process of depositing low optical loss cladding material for waveguide passivation is of critical importance.

A long-standing challenge for low-loss silicon dioxide cladding deposition is the absorption from the second vibrational overtone of OH bonds, which manifests as a strong peak around 1380 nm with a long tail into longer wavelengths [4]. This absorption peak is known in the fiber communication community as the water peak and originates from the hydrogen impurity trapped in the film from the commonly used silicon precursors such as SiH<sub>4</sub>, SiH<sub>2</sub>Cl<sub>2</sub>, and Si(OC<sub>2</sub>H<sub>5</sub>)<sub>4</sub> (TEOS) in the chemical vapor deposition processes.

This notorious absorption peak can only be removed from the deposited film by anneals at very high temperatures (usually >1000 °C), driving out the hydrogen. However, all of these platforms have a low tolerance for process temperature, fundamentally limited by the thermal expansion mismatch, decomposition of material or the Curie temperature for ferroelectrics. As a result, those novel materials are not compatible with current low absorption loss deposition methods, which requires long anneals at very high temperatures.

Here we present an inductively coupled plasma-enhanced chemical vapor deposition (ICPCVD) (Fig 1(a)) inspired by the modified chemical vapor deposition (MCVD) process used in optical fiber preform fabrication. In this process, low-loss SiO<sub>2</sub> free from hydrogen absorption is directly deposited at low temperature with SiCl<sub>4</sub> as the silicon precursor and O<sub>2</sub> as oxidizer. Neither of the precursors contains isotopes of hydrogen, which provides an avenue to produce a completely hydrogen-free SiO<sub>2</sub> film at a low cost, without using the expensive deuterated silicon precursors [8]. The elimination of the OH absorption not only reduces the loss in the technologically important S and C telecommunication bands but also enables operation in the very wide low-loss window spanning the entire 1260 nm to 1620 nm spectrum. This wide low-loss band can enable novel applications such as wide-band parametric amplifiers and frequency comb generators.

## 2. Experimental Results

We measure the surface roughness (Fig 1(c)) and infrared absorption (Fig 1(d)) of the deposited films. An impressively smooth top surface (RMS < 250 pm) after 1.8 μm deposition shows the potential for lowering the scattering loss and compatibility for further heterogeneous integration by direct bonding.

To evaluate the material loss of SiO<sub>2</sub> cladding film deposited with this novel ICPCVD process, we deposit a ~1.5 μm layer on top of Si<sub>3</sub>N<sub>4</sub> ring resonators (Fig 1(b)) as the top cladding and compare the measured resonance linewidth with resonators fabricated with established processes. We use low confinement Si<sub>3</sub>N<sub>4</sub> ring resonators with 200 nm × 5 μm nitride cross-section and 50 GHz free spectral range.

For the TE fundamental mode, ~23% of total optical intensity is distributed in the top cladding (Fig. 2(a)). The Si<sub>3</sub>N<sub>4</sub> ring resonators are fabricated by depositing stoichiometric LPCVD Si<sub>3</sub>N<sub>4</sub> on silicon wafers with 7.2 μm wet oxide layer, defining waveguides by deep ultra-violet lithography, patterning the Si<sub>3</sub>N<sub>4</sub> layer by reactive ion etching, and annealing at 1200 °C for 11 h before cladding deposition or die separation. As a comparison, one of

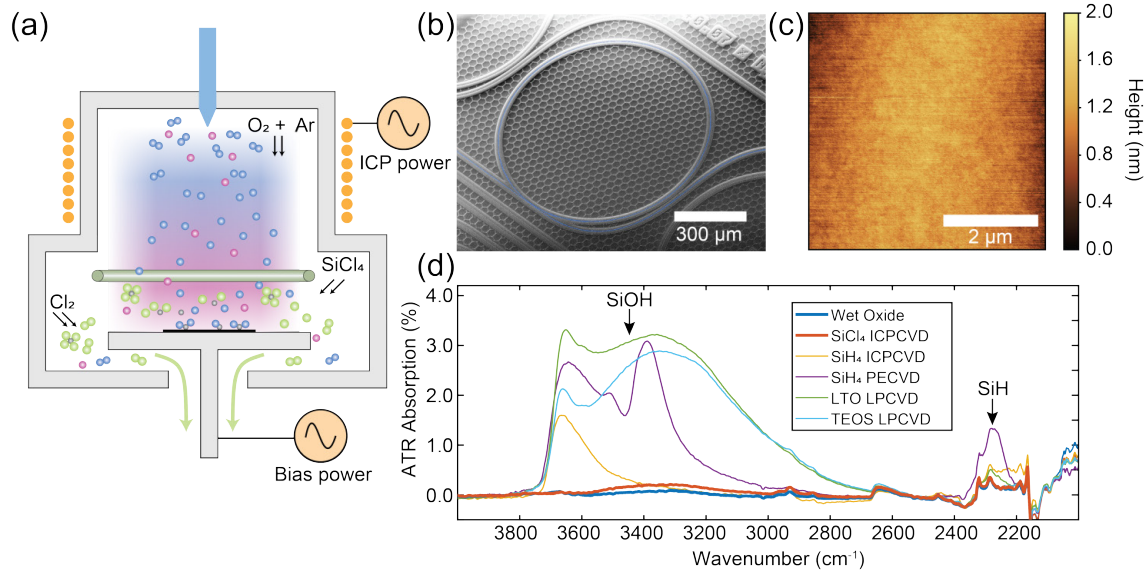


**Fig. 1. Deposition of high-quality  $\text{SiO}_2$  films by  $\text{SiCl}_4$  based ICPCVD.** (a) Schematic of the ICPCVD reactor and the deposition process. (b) Scanning electron microscopy (SEM) image of the low confinement  $\text{Si}_3\text{N}_4$  waveguide resonator. (c) Atomic force microscopy (AFM) height map of the film deposited on a flat substrate. (d) Fourier transform infrared (FTIR) absorption spectrum of  $\text{SiO}_2$  film by  $\text{SiCl}_4$  ICPCVD, in comparison to films created by other methods. LTO: low temperature oxide process.

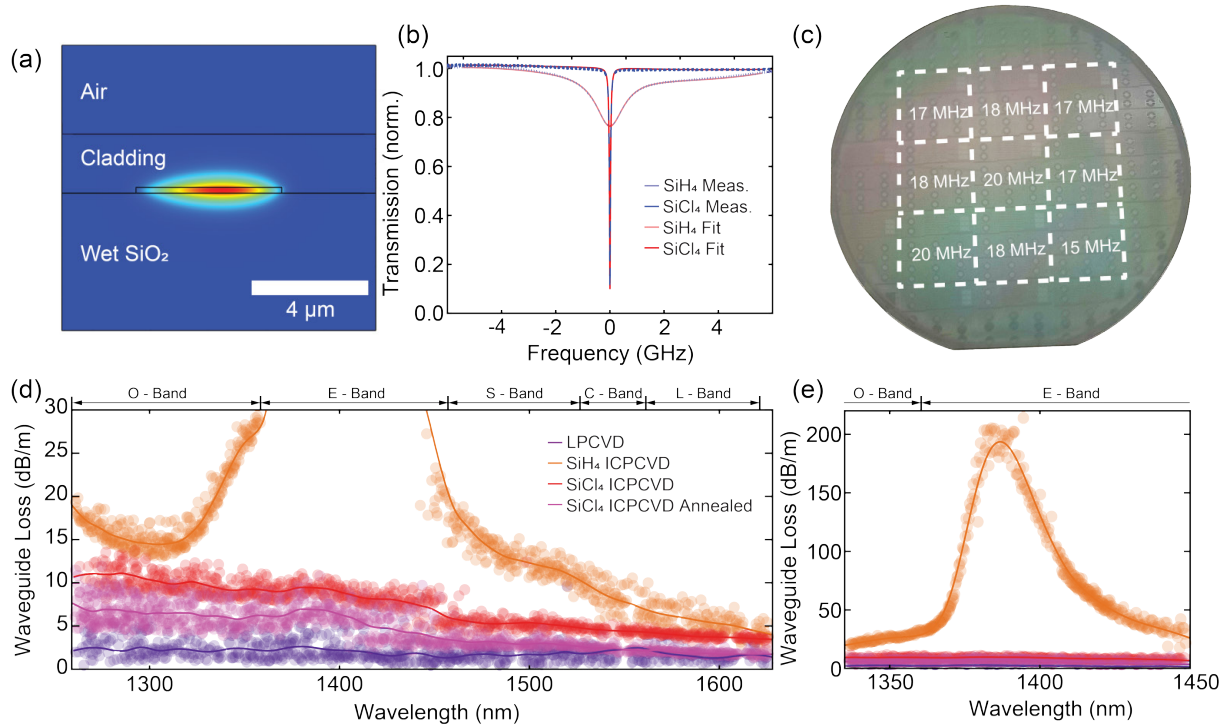


**Fig. 2. Characterization of the novel  $\text{SiCl}_4$  based  $\text{SiO}_2$  cladding.** (a) Cross-section and the optical mode of the  $\text{Si}_3\text{N}_4$  ring resonators used as loss probe. (b) Comparison of typical resonance linewidths of resonators cladded by  $\text{SiCl}_4$  based  $\text{SiO}_2$  and  $\text{SiH}_4$  based  $\text{SiO}_2$  near the OH absorption peak. Center frequencies for the  $\text{SiCl}_4$  and the  $\text{SiH}_4$  one are 216.88 THz and 216.77 THz, respectively. (c) Map of the median intrinsic linewidths around 1550 nm on different stepping fields of a cladded 4-inch wafer (D143.01). (d) and (e) Waveguide losses of the resonators cladded with annealed LPCVD  $\text{SiO}_2$ ,  $\text{SiH}_4$  based ICPCVD and  $\text{SiCl}_4$  based ICPCVD as functions of frequency. The optical communication wavelength bands are marked on the axis.

the wafers is cladded by a well-established LPCVD oxide process with TEOS and  $\text{SiH}_4$  precursors and following 11 h annealing at 1200 °C to fully remove hydrogen impurities and densify the film. Although the baseline process

is known to yield a very low material loss, the requirement of extensive annealing limits its application. For the new ICPCVD process, the deposition is performed in a Oxford Instrument PlasmaPro 100 ICPCVD tool at 300 °C plate temperature. The higher plasma density in the ICP reactor can promote the disassociation of SiCl<sub>4</sub> molecules and accelerate the formation of SiO<sub>2</sub> film. A very high deposition rate of > 40 nm/min can be achieved in certain process conditions. Elemental analysis by X-ray fluorescence spectroscopy indicates the deposited film is doped with Cl. For comparison, another sample is deposited with SiH<sub>4</sub> and O<sub>2</sub> precursors in the same tool, also at 300 °C.

Fig. 2(c) shows a wafer map of the optical loss of the cladded resonators. While the reference ICPCVD film deposited with SiH<sub>4</sub> and O<sub>2</sub> shows a very strong absorption peak at 1380 nm and an additional peak at 1530 nm (caused by SiH bonds [10]), the hydrogen absorption peaks are hardly discernible for the SiCl<sub>4</sub> based film (Fig. 2(d) and (e)). Conservatively including the higher scattering loss of the thinner ICPCVD film, the estimated material loss of the SiO<sub>2</sub> film from SiCl<sub>4</sub> is only 12 dB m<sup>-1</sup> higher than the baseline LPCVD process at 1550 nm. A low waveguide loss is maintained across the entire laser sweep range of 1260 nm to 1625 nm. We also note that for devices that can tolerate 1 h annealing at 500 °C, the loss of cladded waveguides can be further reduced.

### 3. Conclusion

In summary, our work demonstrated a novel PECVD process allowing low-temperature deposition of low-loss SiO<sub>2</sub> cladding, which is essential for the passivation of emerging integrated photonics platforms with low thermal budgets including LiNbO<sub>3</sub> on insulator and III-V semiconductor based photonic integrated circuits.

### 4. Acknowledgement

This work was supported by contract W911NF2120248 (NINJA) from the Defense Advanced Research Projects Agency (DARPA), Microsystems Technology Office (MTO). This was further supported by the EU H2020 research and innovation program under grant No. 965124 (FEMTOCHIP). The samples were fabricated in the EPFL center of MicroNanoTechnology (CMi). We thank Cuenod Blaise for assistance in the process development.

### References

1. D. Zhu *et al.*, "Integrated photonics on thin-film lithium niobate," *Adv. Opt. Photon.*, **13**, 242–352 (2021).
2. L. Chang *et al.*, "Ultra-efficient frequency comb generation in AlGaAs-on-insulator microresonators," *Nat. Commun.*, **11**, 1331 (2020).
3. H. Jung *et al.*, "Tantala Kerr nonlinear integrated photonics," *Optica*, **8**, 811–817 (2021).
4. J. Stone and G. E. Walrafen, "Overtone vibrations of OH groups in fused silica optical fibers," *J. Chem. Phys.*, **76**, 1712–1722 (1982).
5. J. Liu *et al.*, "High-yield, wafer-scale fabrication of ultralow-loss, dispersion-engineered silicon nitride photonic circuits," *Nat. Commun.*, **12**, 2236 (2021).
6. I. H. Malitson, "Interspecimen Comparison of the Refractive Index of Fused Silica," *JOSA* **55**, 1205-1209 (1965)
7. R. Maurer, "Method of producing glass for optical waveguides," United States patent US3791714A (February 12, 1974).
8. W. Jin *et al.*, "Deuterated silicon dioxide for heterogeneous integration of ultra-low-loss waveguides," *Opt. Lett.*, **45**, 3340–3343 (2020).
9. H. Takeuchi *et al.*, "Thermal budget limits of quarter-micrometer foundry CMOS for post-processing MEMS devices," *IEEE Transactions on Electron Devices*, **52**, 2081–2086 (2005).
10. P. J. Lemaire and M. D. Decoteau, "Optical Spectra of Silica Core Optical Fibers Exposed to Hydrogen," *MRS Proceedings*, **88**, 225–232 (1986).